

Distributed feedback–distributed Bragg reflector coupled cavity laser with a Ti:(Fe:)Er:LiNbO₃ waveguide

Bijoy K. Das,* Raimund Ricken, Viktor Quiring, Hubertus Suche, and Wolfgang Sohler

Applied Physics, University of Paderborn, Paderborn 33098, Germany

Received August 18, 2003

A thermally fixed photorefractive Bragg grating is written in a single-mode Ti:Fe:Er:LiNbO₃ channel waveguide and used to develop a distributed feedback–distributed Bragg reflector coupled cavity laser with a second broadband dielectric cavity mirror. The optically pumped ($\lambda_p = 1480$ nm, $P = 130$ mW) laser emits in single-frequency operation as much as 8 mW at $\lambda = 1557.2$ nm with a slope efficiency of $\sim 22\%$. The laser wavelength can be thermo-optically and electro-optically tuned over 100 pm. © 2004 Optical Society of America

OCIS codes: 130.3120, 130.3730, 140.3580, 140.5680.

Recently, integrated Er-doped LiNbO₃ single-frequency lasers with Ti-indiffused channel waveguides were developed. Their cavity is formed by a dielectric end-face mirror and a photorefractive Bragg grating¹ or by two photorefractive gratings in Fe-doped sections outside the waveguide amplifier.² The linewidth of such distributed Bragg reflector (DBR) lasers can be as low as 10 kHz.³ Therefore they are attractive devices for wavelength division multiplexing systems and for interferometric instrumentation. Also recently, a distributed feedback (DFB) laser was developed with a photorefractive grating written in the gain section of a Ti:Fe:Er:LiNbO₃ waveguide.^{4–6}

In this Letter we demonstrate for the first time to our knowledge a DFB–DBR coupled cavity laser with a Ti:(Fe:)Er:LiNbO₃ waveguide and a grating in the gain section itself (see Fig. 1). The laser cavity is comprised of a thermally fixed photorefractive Bragg grating in the Ti:Fe:Er:LiNbO₃ waveguide section close to one end face of the sample and a broadband dielectric multilayer high-reflection mirror (HR coating) on the other end face. For laser operation the pump light ($\lambda = 1480$ nm) is fed into the laser resonator through the grating by the common branch of a fiber-optic wavelength division demultiplexer. The laser output is extracted through the second branch of the wavelength division demultiplexer and isolated to protect the laser from optical feedback.

The laser was fabricated in the surface of a 65-mm-long, 12-mm-wide, 1-mm-thick optical grade X-cut LiNbO₃ crystal. The Z (optical) axis was parallel to the propagation direction of the optical waveguide. The fabrication procedure started with an indiffusion of a 20-nm-thick Er layer at 1130 °C for 140 h. Subsequently, a 15-mm-long area close to one end of the substrate, where the Bragg grating was to be fabricated later, was doped with Fe (37-nm-thick film indiffused at 1060 °C for 72 h) to enhance the photorefractive sensitivity. Afterwards, a 7- μ m-wide, 100-nm-thick Ti stripe aligned parallel to the Z axis was indiffused at 1060 °C for 7.5 h to form the optical channel guide (single mode at $\lambda = 1480$ and 1550 nm). The sample was then annealed at 500 °C for 5 hr in flowing Ar (0.5 l/min) that was bubbled

through water at 80 °C to enhance the Fe²⁺/Fe³⁺ ratio and the proton concentration in the surface layer. Both are necessary conditions for the fabrication of a fixed (ionic) photorefractive grating.⁷ Afterwards, the polished end faces were antireflection coated on the Fe-doped side of the substrate and high-reflection coated on the other side, respectively.

Finally, a 14-mm-long photorefractive Bragg grating was written in the Fe-doped waveguide section with a holographic setup with an Ar-ion laser ($\lambda = 488$ nm, $P = 1$ W). It was fabricated at 180 °C by a holographic exposure for 4 min, followed by a rapid cooling of the sample to room temperature to obtain a fixed ionic (protonic) grating of 352-nm periodicity. It was developed by uniform illumination with blue light either from an Ar laser or an array of blue LEDs (details are reported elsewhere²).

To measure the transmission characteristics of the grating, an optical spectrum analyzer of 10-pm resolution was used to monitor the transmitted amplified spontaneous emission of an Er-doped fiber amplifier through the grating. Some results are given in Fig. 2. As much as 90% peak reflectivity (deduced from the transmission spectrum) could be achieved if the Ar laser ($\lambda = 488$ nm, $I = 250$ mW/cm², 20-min exposure time) was used to develop the ionic grating. After development, the grating slowly decayed because of the dark conductivity of residual free electrons but could be refreshed to as high as 75% peak reflectivity by an array of eight blue

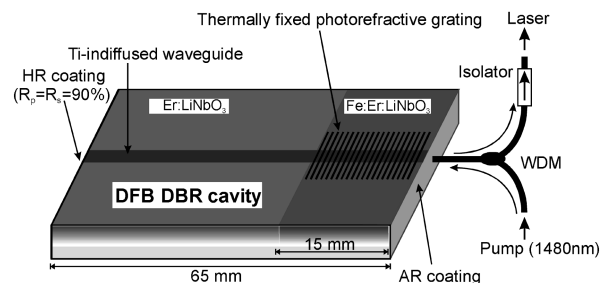


Fig. 1. Schematic structure of DFB–DBR coupled cavity laser in operation: AR, antireflection; WDM, wavelength division demultiplexer.

LEDs within 30 min. The spectral half-width of the polarization-independent grating response was 70 pm (~ 8.5 GHz). Moreover, during laser operation a stabilization of the grating response at $\sim 30\%$ reflectivity was observed even without any additional blue illumination from outside. This favorable self-stabilization was probably caused by the green upconversion light produced in the Er-doped grating itself.

The specific laser investigated in detail had a grating of $\sim 40\%$ reflectivity. It was pumped by a fiber-coupled laser diode of 1480-nm wavelength. At ~ 80 mW of launched pump power, oscillation began in a pure DBR mode of operation with a low slope efficiency of only 2.5% (see Fig. 3). In this mode the emission frequency of the laser was determined by the frequency of that DBR cavity mode ($\Delta\nu_{\text{DBR}} \approx 1.4$ GHz), which was closest to the reflectivity maximum of the grating. Slightly above threshold, single-frequency emission of <185 -MHz linewidth was observed with a Fabry–Perot spectrum analyzer at 1557.2-nm wavelength [the true linewidth is probably ≤ 10 kHz (Ref. 3)] before oscillation in more than one DBR mode of 1.4-GHz frequency spacing set in.

At ~ 90 mW of launched pump power a DFB–DBR coupled mode of laser oscillation set in. In this regime a maximum output power of 8 mW was obtained at 130 mW of pump power. This corresponds to a slope efficiency of $\sim 22\%$ (see Fig. 3). In contrast to the DBR mode of operation, simultaneous emission at two frequencies separated by ~ 3.8 GHz was observed [see Figs. 4(a) and 5(a)]. Both the threshold pump power and the observed frequency spacing of the two lasing modes were smaller than the theoretical results for a pure DFB laser,⁸ clearly indicating an influence of the integrated amplifier section^{4,9} and the cavity formed by the high-reflector dielectric mirror and the grating. The coupled mode of laser operation is determined by the amplified spontaneous emission at the two distinguished frequencies of the DFB laser and amplifier combination in the wings of the reflectivity spectrum of the 14-mm-long amplifying grating. They determined the laser oscillation frequencies in the longer DBR cavity, if two DBR modes are resonant or (symmetrically) close to resonance with the two DFB laser and amplifier modes.

However, the DBR cavity modes can shift as a function of temperature ($\Delta\nu_{\text{DBR}}/\Delta T \approx 700$ MHz/ $^{\circ}\text{C}$), leading to a resonance of one of the two DFB frequencies with only one DBR cavity mode, resulting in single-frequency emission [see Figs. 4(b) and 5(b)].

The observed emission characteristics of the DFB–DBR coupled cavity laser (shown in Fig. 4) is schematically explained in Fig. 5. In this figure the comb of possible DBR cavity modes (dotted vertical lines) and the frequencies of the two DFB modes (solid vertical lines) are sketched for different temperatures along with the calculated reflectivity response of the pumped and therefore slightly amplifying grating. Laser oscillation starts at the two distinguished DFB modes simultaneously if these resonances at least partially overlap with two DBR modes, as shown in Fig. 5(a). On the other hand, single-frequency laser

emission is achieved if only one DFB mode overlaps with only one DBR mode, as shown in Fig. 5(b).

During the single-frequency operation the laser emission wavelength can be tuned by temperature and electro-optic tuning. A change in the sample temperature causes a change in the effective cavity length as well as of the period of the grating structure, resulting in a corresponding change in the laser emission wavelength. The tuning slope observed was ~ 5 pm/ $^{\circ}\text{C}$; the tuning range was ~ 100 pm, which was

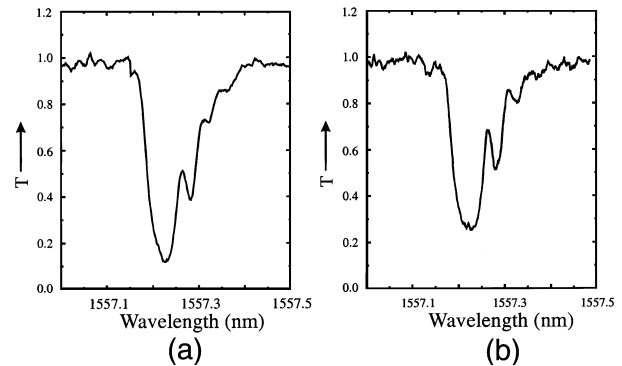


Fig. 2. Normalized transmission characteristics of a fixed ionic grating in TE polarization (a) developed by homogeneous Ar laser illumination (250 mW/cm²) and (b) developed by illumination from an array of eight blue LEDs.

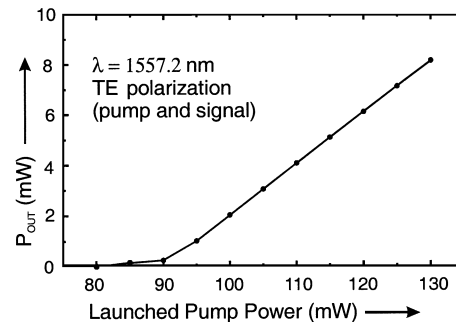


Fig. 3. DFB–DBR coupled cavity laser output power versus launched pump power.

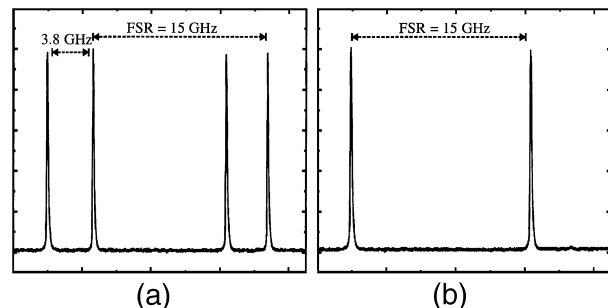


Fig. 4. Measured Fabry–Perot spectra of the laser emission in the DFB–DBR coupled mode of operation at two slightly different temperatures. (a) Simultaneous emission of the two DFB modes with frequencies symmetrical to a pair of DBR cavity modes. (b) Single-frequency emission of one DFB mode in resonance with one DBR cavity mode. FSR, free spectral range of the Fabry–Perot spectrum analyzer.

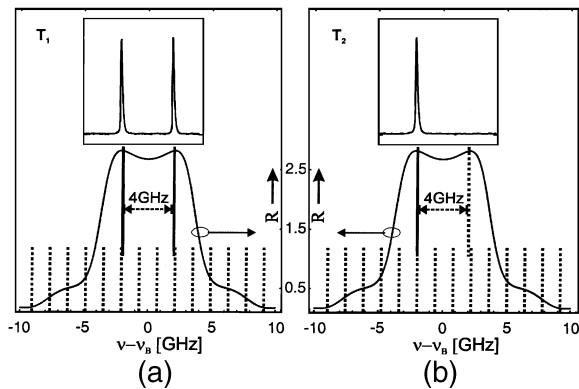


Fig. 5. Schematic explanation of the DFB-DBR coupled cavity laser emission with the calculated reflectivity response of the pumped and therefore slightly amplifying grating, frequency comb of possible DBR cavity modes (dotted vertical lines), and the two frequencies of the distinguished DFB modes (solid vertical lines). (a) Simultaneous emission of the two DFB modes with frequencies symmetrical to a pair of DBR cavity modes. Inset, observed Fabry-Perot spectrum. (b) Single-frequency emission of one DFB mode in resonance with one DBR cavity mode. Inset, observed Fabry-Perot spectrum.

determined by the spectral width of the grating. To demonstrate electro-optic tuning, we integrated two parallel electrodes that were separated by $15\ \mu\text{m}$ on both sides of the grating of a similar laser operating at $\lambda \sim 1561.5\ \text{nm}$. A tuning slope of $\sim 0.75\ \text{pm/V}$ was observed in a tuning range of $\sim 75\ \text{pm}$.

In conclusion, the first, to our knowledge, DFB-DBR coupled cavity laser with a Ti:Fe:Er:LiNbO₃ channel guide has been demonstrated. As much as 8 mW of laser output power was obtained at 1557.2-nm wavelength at a pump power level of 130 mW ($\lambda_p = 1480\ \text{nm}$, $P_p = 130\ \text{mW}$). The laser emits either two modes simultaneously, which is specific to a DFB laser structure with a homogeneous grating, or only one mode if it is in resonance with

one of the DBR cavity modes. This behavior is qualitatively explained. To obtain single frequency operation, a coupled DFB-DBR cavity can be an attractive alternative to the introduction of a $\lambda/4$ phase shift within the grating structure as routinely used in single-frequency semiconductor DFB lasers.

This work was supported by the Deutsche Forschungsgemeinschaft as one project of the research group Integrated Optics in Lithium Niobate: New Devices, Circuits and Applications. B. K. Das's e-mail address is b.das@ele.eng.osaka-u.ac.jp.

*Present address, Integrated Optoelectronics, Department of Electronics Engineering, Graduate School of Engineering, Osaka University, 2-1 Yamada-Oka, Suita, Osaka, 565-0871, Japan.

References

1. C. Becker, A. Greiner, T. Oesselke, A. Pape, W. Sohler, and H. Suche, *Opt. Lett.* **23**, 1194 (1998).
2. B. K. Das, H. Suche, and W. Sohler, *Appl. Phys. B* **73**, 439 (2001).
3. I. Baumann, S. Bosso, R. Brinkmann, R. Corsini, M. Dinand, A. Greiner, K. Schäfer, J. Söchtig, W. Sohler, H. Suche, and R. Wessel, *IEEE J. Sel. Top. Quantum Electron.* **2**, 355 (1996).
4. B. K. Das, R. Ricken, and W. Sohler, in *Conference on Lasers and Electro-Optics (CLEO)*, Vol. 73 of OSA Trends in Optics and Photonics Series (Optical Society of America, Washington, D.C., 2002), postdeadline paper CPDB-11.
5. B. K. Das, R. Ricken, and W. Sohler, *Appl. Phys. Lett.* **82**, 1515 (2003).
6. B. K. Das, C. Becker, T. Oesselke, R. Ricken, V. Quiring, H. Suche, and W. Sohler, *Proc. SPIE* **4944**, 41 (2003).
7. K. Buse, S. Breer, K. Peithmann, S. Kapphan, M. Gao, and E. Krätzig, *Phys. Rev. B* **56**, 1225 (1997).
8. A. Yariv, *Quantum Electronics* (Wiley, New York, 1988), Chap. 22.
9. S. Wang, R. F. Codero, and C. Tseng, *J. Appl. Phys.* **45**, 3975 (1974).